

Article

Controlling of Chemical Bonding Structure, Wettability, Optical Characteristics of SiCN:H (SiC:H) Films Produced by PECVD Using Tetramethylsilane and Ammonia Mixture

Evgeniya Ermakova ^{1,*}, Alexey Kolodin ², Anastasiya Fedorenko ³, Irina Yushina ¹, Vladimir Shayapov ¹, Eugene Maksimovskiy ¹ and Marina Kosinova ^{1,*} 

¹ Laboratory of Functional Films and Coatings, Nikolaev Institute of Inorganic Chemistry, SB RAS, Novosibirsk 630090, Russia

² Laboratory of Extraction, Nikolaev Institute of Inorganic Chemistry, SB RAS, Novosibirsk 630090, Russia

³ Laboratory of Nanomaterials, Nikolaev Institute of Inorganic Chemistry, SB RAS, Novosibirsk 630090, Russia

* Correspondence: ermakova@niic.nsc.ru (E.E.); marina@niic.nsc.ru (M.K.)

Abstract: PECVD SiC:H (SiCN:H) films were produced using tetramethylsilane (TMS) as a precursor in a mixture with inert helium or ammonia as a source of nitrogen. Mild plasma conditions were chosen in order to prevent the complete decomposition of the precursor molecules and promote the incorporation of the fragments of precursor into the film structure. The effect of deposition temperature and composition of gas mixture on the chemical bonding structure, elemental composition, deposition rate, and optical properties (transmittance, optical bandgap, and refractive index) of films have been examined. Use of the chosen deposition conditions allowed them to reach a relatively high deposition rate (up to 33 nm/min), compared with films produced in high plasma power conditions. Use of ammonia as an additional gas led to effective incorporation of N atoms in the films. The composition of the films moved from SiC:H to SiN:H with increasing of ammonia content to $P(\text{NH}_3)/P(\text{TMS}) = 1$. The refractive index and optical bandgap of the films varied in the range of 1.55–2.08 and 3.0–5.2 eV, correspondingly, depending on the film composition and chemical bonding structure. The effect of treatment of SiCN films deposited at 400 °C by plasma of He, O₂ or NH₃ were studied by X-ray photoelectron spectroscopy, atomic force microscopy, and contact angle measurements. It was shown that plasma treatment significantly changes the surface characteristics. The water contact angle of the film was changed from 71 to 37° after exposure in the plasma conditions.

Keywords: silicon carbonitride (SiCN) coatings; PECVD; thin film; tetramethylsilane (TMS); refractive index; optical bandgap; contact angle



Citation: Ermakova, E.; Kolodin, A.; Fedorenko, A.; Yushina, I.; Shayapov, V.; Maksimovskiy, E.; Kosinova, M. Controlling of Chemical Bonding Structure, Wettability, Optical Characteristics of SiCN:H (SiC:H) Films Produced by PECVD Using Tetramethylsilane and Ammonia Mixture. *Coatings* **2023**, *13*, 310. <https://doi.org/10.3390/coatings13020310>

Academic Editor: Angela De Bonis

Received: 29 December 2022

Revised: 23 January 2023

Accepted: 26 January 2023

Published: 30 January 2023



Copyright: © 2023 by the authors. Licensee MDPI, Basel, Switzerland. This article is an open access article distributed under the terms and conditions of the Creative Commons Attribution (CC BY) license (<https://creativecommons.org/licenses/by/4.0/>).

1. Introduction

Silicon carbonitride films are attractive coatings for advanced technology due to their favorable physical characteristics, including optical properties. Due to their tunable refractive index and bandgap, SiCN coatings are perspective materials for solar cell technology, UV detectors operated at high temperatures, integrated photonics and solid state lighting [1–4]. Plasma enhanced chemical vapor deposition (PECVD) is one of the most common deposition techniques for SiC:H (SiCN:H) films formation that allows for producing high-quality films with good adhesion to the substrate, and also lowering the temperature required for precursor activation and film formation. Use of the various organosilicon precursors leads to preventing the involvement in CVD processes of flammable and toxic silane. Concurrently, the presence of the fragments with different combinations of Si–C, Si–N and C–N bonds in the precursor molecule seems to be an effective way to control the chemical bonding structure of the films. The variety of organosilicon precursors includes commercially available compounds, such as tetramethylsilane [5–7], hexamethyldisilazane [8,9], and tetramethyldisilazane [10,11]. The novel substances of organosilanes, silazanes, aminosilazanes or carbodiimides, such as hexamethylcyclotrisilazane [12],

bis(trimethylsilyl)ethylamine [13], bis(trimethylsilyl)phenylamine [14], 1,3-bis(dimethylsilyl)-2,2,4,4-tetramethylcyclodisilazane [12], N-methyl-aza-2.2.4-trimethylsilacyclopentane [15], and bis(tetramethylguanidine)dimethylsilane [16], (dimethylamino)dimethylsilane [17], tris(dimethylamino)silane [17], bis(dimethylamino)methylsilane [18], methyltris(diethylamino)silane [19], tris(diethylamino)silane [20], and tris(dimethylamino)silane [21], bis(trimethylsilyl)carbodiimide [22] and dimethyl(2,2-dimethylhydrazino)silane [23], are also regarded as potential precursors for silicon carbonitride film synthesis for different applications. In the review [24], we considered the relationship between the structure of the precursor molecule and the nature of the bonds present in the films deposited with its participation. Indeed, numerous publications show that the architecture of the precursor affects significantly the chemical bonding structure of the films. However, the approach of a single-source precursor has a limitation on the composition of the deposited films, and results in a low concentration of nitrogen observed. The most effective way to control the nitrogen content in a wide range is to introduce additional reactive gas (N_2 , NH_3) into the CVD reactor. However, in this case, the formation of nitrogen-containing bonds is uncontrollable and strongly depends on the synthesis conditions and needs further investigation.

In this work, tetramethylsilane $Si(CH_3)_4$ (TMS) was chosen as precursor for film preparation. The advantage of this compound as a CVD precursor is its high vapor pressure, allowing high growth rates, combined with the ability to control the composition of films in a wide range by varying additional gases and changing the conditions of synthesis, and also safe operation, compared to pyrophoric silane. Because of this, TMS has found application in the area of thin film production. It has been shown that SiC:H sublayers obtained using TMS promote an increase in the adhesion of DLC films to steel, as well as an increase in the hardness of the entire structure [25,26]. CH:Si films obtained using a mixture of TMS and acetylene showed corrosion resistance to nitric acid [27]. The silicon nitride coating obtained using a mixture of TMS and ammonia had passivating properties and also contributed to the stabilization of the aluminum oxide sublayer during operation at elevated temperatures [28]. Silicon carbonitride layers using from a mixture of TMS and ammonia under the conditions of MW PECVD synthesis possessed such mechanical properties as hardness of up to 12 GPa and a Young's modulus of up to 120 GPa [29]. More information on the composition, chemical bonding structure and properties of the Si-C-N-H films produced using TMS as a precursor is given in Table 1. It is worth noting that high plasma power of 50–1500 W was used in the publications mentioned above. The optical, mechanical, and dielectric properties of the films were studied.

Table 1. The literature data on Si–C–N films synthesis and characterization using TMS as a precursor.

Film	Gas Mixture	Deposition Conditions	Elemental Composition and Binding Structure	Properties	Ref.
SiN _x :H	TMS + NH ₃	PECVD; P = 1200 W; T = 120 °C; u(TMS) = 5–35 sccm; u(total) = 60 sccm. Post-annealing at 450 °C	Si–N is dominant at u(TMS) > 25 sccm, the presence of N–H, Si–H, Si–C, C–H	Rear passivation layer. SiN _x :H films deposited at 30 and 35 sccm have dense structure, stable to the etching during storage in HCl.	[28]
SiCN:H	TMS + NH ₃	MW-PECVD *; P = 1000 W; T = 400 °C; r = u(NH ₃)/u(TMS) = 11.2 and 1.5	r = 11.2: Si _{0.5} C _{0.3} N _{0.2} , Si–N bond is dominant by XPS; r = 1.5: Si _{0.36} C _{0.55} N _{0.08} , Si–C + Si–N bonds by XPS	AFM roughness increases with growth of TMS percentage in the gas flow	[5]
SiC _x :H, SiC _x N _y :H	TMS + Ar, TMS + N ₂	ICP CVD *; P = 50–500W, T = 50–450 °C, p(Ar or N ₂) = 3.5–4 × 10 ^{−3} Torr; p(TMS) = 0–3 × 10 ^{−3} Torr	Si _{0.05} C _{0.6} N _{0.2} O _{0.2} with predominant Si–C (Si–CHx–Si) binding	Optical bandgap: 2.8–3 eV at P > 100 W, 3.6 eV at P = 50 W, T = 200 °C, TMS/N ₂ = 0.6	[6]
SiCN:H	TMS + N ₂	ECR CVD *; P = 200 W; u(N ₂)/u(TMS) = 0.7–1.3	Si _{0.45} C _{0.12} N _{0.3} O _{0.3} at r = 1.3 Si _{0.55} C _{0.02} N _{0.45} O _{0.02} at r = 0.7 Si–C, Si–N, C–N, Si–O and C–C bonds, Si–N dominates	H = 17.6–27.6 GPa E = 163.7–230.7 GPa	[7]
SiC _x N _y :H	TMS + NH ₃	PECVD; P = 1500 W; T = 400 °C; r = [TMS]/[NH ₃] = 0.015–0.5	Si _{0.43} C _{0.11} N _{0.47} at r = 0.015 (dominant is Si–N); Si _{0.34} C _{0.44} N _{0.22} at r = 0.5 (dominant is Si–C)	Refractive index 1.85–2.1, growth rate 0.49–22 nm/min, passivation behavior: τ _{eff} = 420 μs	[30]
SiCNH	TMS + NH ₃	PECVD; V _{DC} = 50 V; T = 350 °C; u(NH ₃) = 26sccm; u(TMS) = 6 sccm	r(TMS/NH ₃) = 0.23 led to SiN:H films deposition	Refractive index (640 nm) = 1.75	[31]
α-SiCN:H	TMS + NH ₃	PECVD; 350 °C	Si/N = 2.06, Si–C is dominant	Dielectric constant 5.68. Tested as Diffusion Barrier Film	[32]
SiC, SiCN	TMS + NH ₃	PECVD; V = −500 V; T = 180 °C; r = u(NH ₃)/u(TMS) = 0 or 1	Dominant bonds: Si–C for r = 0; Si–N for r = 1	Anti-corrosion properties in NaCl-H ₂ O: SiCN—more effective corrosion resistance; tribology: SiCN layer degraded after 200 cycles	[33]

* Abbreviations: MW-PECVD—microwave plasma enhanced chemical vapor deposition; ICP CVD—inductively coupled plasma enhanced chemical vapor deposition; ECR CVD—electron cyclotron resonance chemical vapor deposition. Variables: P—plasma power; u—gas flow; T—deposition temperature; p—partial pressure; V_{DC}—self-bias voltage; τ_{eff}—charge carrier effective lifetimes.

In this study, we performed the synthesis of SiC:H (SiCN:H) films in mild conditions using low plasma power of 20 W. It seems to result in less fragmentation of the precursor molecule with preservation of Si–C bonds. The optical properties of the films, such as refractive index, transmittance, and optical bandgap, and their dependence on deposition conditions and films composition and bonding structure were investigated. Additionally, the tuning of SiCN:H film surface bonding structure, surface topology and wettability by short plasma treatment in different environments (He, O₂, NH₃) have been studied.

2. Materials and Methods

2.1. Materials

Tetramethylsilane Si(CH₃)₄ (99.9%, Alfa Aesar, Heysham, UK) was utilized as precursor for SiC:H (SiCN:H) films synthesis. High-purity helium and ammonia were applied as plasma-forming gases.

The films were deposited on the polished silicon (100) and germanium (110) wafers, and fused silica slides. All of them were preliminarily degreased by consequently boiling in trichlorethylene and acetone, and then washed in deionized water. Si substrates were then treated in ammonia–peroxide and hydrochloric–peroxide solution. The SiO₂ layer was removed by HF solution. Ge substrates after degreasing were treated in HNO₃/HF/HCOOH solution. After final cleaning in deionized water, the films were dried in a flow of nitrogen. All reagents had ‘extra pure’ degree of purity.

2.2. PECVD and Surface Modification

SiC:H (SiCN:H) films were deposited by PECVD technique. The in-house-built CVD equipment is described in detail in [34]. The process was carried out in a tunnel-type quartz reactor with a length of 0.5 m and a diameter of 0.3 m. The size of the substrate holder was 15 × 30 mm. The liquid precursor TMS was placed in a glass ampoule and kept at room temperature (23 °C). The vapor was delivered into the reactor chamber through the system of valves. The partial pressure of the substance was regulated by means of a control valve. Stability of vapor pressure was confirmed by measuring it before and after PECVD experiment. The synthetic experiments on SiC:H (SiCN:H) films preparation were carried out at the following parameters (Table 2). The film growth experiments were carried out at substrate temperatures ranging from 100 to 400 °C. Plasma power of 20 W was provided through radio-frequency (RF) plasma source (40.68 MHz). The base pressure in the CVD reactor did not exceed 4×10^{-3} Torr. For two series with variable deposition temperature, partial pressures of precursor vapor and plasma-forming gas (helium or ammonia) were fixed as: for TMS— 1.5×10^{-2} Torr (0.33 sccm), He— 6×10^{-3} Torr (0.13 sccm), NH₃— 6×10^{-3} Torr (0.13 sccm). In experiments to study the effect of ammonia content in the initial gas mixture, the TMS partial pressure was varied from 6×10^{-3} to 1.5×10^{-2} Torr (0.13–0.33 sccm), while the total TMS + NH₃ pressure in all experiments was maintained equal to 2.1×10^{-2} Torr.

The post-deposition surface modifications were applied for the samples of SiCN:H films prepared at 400 °C using TMS + NH₃ mixture (P (NH₃) = 6×10^{-3} Torr (0.13 sccm), P (TMS) = 1.5×10^{-2} Torr (0.33 sccm)). The thickness of the films was 200 nm. After the synthesis the sample was cooled in the vacuum chamber to 100 °C, and in order to perform a detailed comparative experimental study, then treated by He, NH₃ or O₂ plasma. The pressure of the gas was 6×10^{-3} Torr (0.13 sccm), plasma power—20 W. The temperature was kept by controller at 100 °C during the whole experiment in order to prevent the effect of uncontrolled heating of the sample by plasma.

Table 2. Experimental conditions.

Deposition					Treatment				
P(TMS), Torr	Add. Gas	P (Add. Gas), Torr	T, °C	Plasma Power, W	Gas	P, Torr	Plasma Power, W	T, °C	Time, min
1.5×10^{-2}	He	6×10^{-3}	100–400	20			No treatment		
1.5×10^{-2}	NH ₃	6×10^{-3}	100–400	20			No treatment		
1.2×10^{-2}	NH ₃	8×10^{-3}	400	20			No treatment		
1.0×10^{-2}	NH ₃	1.0×10^{-2}	400	20			No treatment		
8×10^{-3}	NH ₃	1.2×10^{-2}	400	20			No treatment		
6×10^{-3}	NH ₃	1.5×10^{-2}	400	20			No treatment		
1.5×10^{-2}	NH ₃	6×10^{-3}	400	20	He	6×10^{-3}	20	100	5
1.5×10^{-2}	NH ₃	6×10^{-3}	400	20	NH ₃	6×10^{-3}	20	100	5
1.5×10^{-2}	NH ₃	6×10^{-3}	400	20	O ₂	6×10^{-3}	20	100	5

2.3. Plasma Characterization

The plasma emission spectra were recorded by multichannel spectrometer “Kolibri-2” (VMK-Optoelectronika, Novosibirsk, Russia). The spectrometer detector consists of a 2580-element linear photodiode array. The spectral resolution was 1 nm in the wavelength range 200 to 1000 nm. Temperature stabilization of the photodiode array was supported by a two-stage Peltier module and digital temperature sensor. Atomic line identification was carried out in correspondence with the NIST atomic line database [35]. Electron excitation temperature was calculated using the ratio of intensities of the two atomic hydrogen spectral lines at 656.3 and 486.1 nm [36].

2.4. Characterization of Chemical Bonding Structure and Composition

XPS and FTIR were applied for chemical bonding structure characterization of the films. FTIR as a bulk method was preferred for analysis of SiC:H (SiCN:H) films, as it allows for minimizing the value of the surface layer that can be degraded during exposure to the ambient conditions, and also gives information on hydrogen-containing bonds content. XPS investigation was performed for the samples treated by plasma to reveal accurately the changes of the film surface.

Fourier Transform Infra-Red (FTIR) spectra of SiC:H (SiCN:H)/Si(100) samples were recorded at room temperature using FTIR-spectrophotometer SCIMITAR FTS 2000 (Digilab, Hopkinton, MA, USA) in transmission mode in the range of 400–4000 cm⁻¹ with a resolution of 2 cm⁻¹. Each spectrum was normalized by the thickness of the film in order to compare the bond intensities. A cleaned silicon substrate, cut from the same plate as the film synthesis substrates, was used to record the FTIR spectra.

XPS analysis was carried out on a FlexPS spectrometer with PHOIBOS 150 analyzer (Specs GmbH, Berlin, Germany) using a non-monochromatic Mg K α excitation radiation. The Casa XPS software (Casa Software Ltd., Teignmouth, UK) was used for data processing. The Si2p, C1s, and N1s spectra were fitted by mixed Gaussian–Lorentzian peaks after subtraction of a Shirley background. The binding energies were calibrated to the C–C component energy of C1s peak at 284.6 eV. The choice of this calibration method was determined by the need to take into account the shift of the lines due to the charging of the samples.

Elemental analysis of SiC:H (SiCN:H)/Ge(110) sample was performed by Scanning Electron Microscope JEOL JSM 6700F (Jeol, Tokyo, Japan) equipped by Energy-Dispersive X-Ray (EDX) analyzer Quantax 200 (Bruker, Berlin, Germany) which was used for at the accelerated voltage of 5 keV in secondary electron mode. In order to exclude the effect of Si substrate to the composition, the films were deposited on the Ge wafers.

2.5. Characterization of Thickness and Optical Properties

The film thickness and refractive index n of the films deposited on Si(100) wafers were determined using monochromic null ellipsometry at a wavelength of 632.8 nm (He–Ne laser). The refractive index and the thickness of the films were calculated from the measured polarization angles ψ and Δ . The deposition rate was calculated by the dividing of film thickness to synthesis time. The values of the refractive index were calculated with an error of 0.03, which is determined by measuring the parameters ψ and Δ , as well as the choice of the initial model of the inverse problem.

Transmittance of the films deposited on SiO₂ substrates was determined using Shimadzu UV–3101PC scanning spectrophotometer (Shimadzu, Kyoto, Japan) in the range of 200–2000 nm with a resolution of 2 nm. The optical bandgap values were estimated from transmittance curves using Tauc's model [37].

2.6. Surface Topology

The AFM study was performed using a Ntegra Prima II atomic force microscope (NT-MDT, Zelenograd, Russia), operating at room temperature in air. The microscope was fitted with HA_NC (A) cantilever (force constant of 17 N/m) run in the semi-contact mode at a scan frequency of 230 kHz. RMS roughness measurements were obtained from the average roughness collected from a 25 μm \times 25 μm area. Image analysis was performed using standard software provided with the instrument.

2.7. Wettability and Free Surface Energy

The measurements of the contact angles on the films were performed on an OCA 15 PRO instrument (Dataphysics, Filderstadt, Germany), equipped with a measuring video system with a USB camera, as well as a fast-measuring lens with an adjustable viewing angle. All measurements were performed under normal conditions in a thermostatic box ($T = 25 \pm 2$ °C and $p = 750$ Torr). The values of the contact angles were measured in the regime of a sessile drop mode with constant droplet volume of ~ 2.0 μL . The calculation of the observed contact angle was carried out according to two algorithms: Ellipse-Fitting, the Young–Laplace algorithm. The final values of the contact angles were calculated as the average of 2–3 measurements in the different regions of the substrate. The calculation of the free surface energy (E_s , mN/m), as well as its polar and dispersion components (E_{sp} and E_{sd}), was carried out using three methods: Neumann, Owens–Wendt, and Wu [38–40]. For this, the values of the contact angles and surface tensions of two test liquids (water and diethylene glycol) with different polarities were used.

3. Results and Discussion

3.1. Effect of Deposition Temperature during the PECVD Process

To study the film formation chemistry, the gas phase (TMS, TMS/He, TMS/NH₃ gas mixtures) was analyzed by optical emission spectroscopy (OES). The obtained information allowed for estimating the value of additional gas and deposition temperature on the chemical bonding structure and composition of the deposited films. Figure 1a presents optical emission spectrum of TMS plasma without additional gases. The spectrum shows hydrogen atomic lines, hydrogen and nitrogen molecular bands, CH and CN free radicals. Thus, decomposition of TMS is accompanied by the detachment of methyl groups and hydrogen atom's appearance from the initial molecule. Nitrogen-containing species originate from residual atmosphere in the CVD reactor. Electron excitation temperature in TMS/He plasma is higher than in TMS/NH₃ plasma (Figure 1b), i.e., helium provides a higher plasma excitation than NH₃ since vibration energy losses are missing.

SiC:H (SiCN:H) films have been synthesized using TMS/He or TMS/NH₃ gas mixtures at the deposition temperature ranging from 100 to 400 °C. Low-power plasma conditions have been applied in order to reach the incomplete decomposition of the organosilicon precursor with a preservation of Si–C bonds. The chemical bonding structure, elemental composition, growth rate, and optical properties have been studied.

Figure 2 presents FTIR spectra (Figure 2a,b) and elemental composition (Figure 2c,d) of the films deposited using TMS/He (Figure 2a,c) and TMS/NH₃ (Figure 2b,d) mixtures at various deposition temperatures. In order to compare the intensities of the bands, each spectrum has been divided by the thickness of the sample.

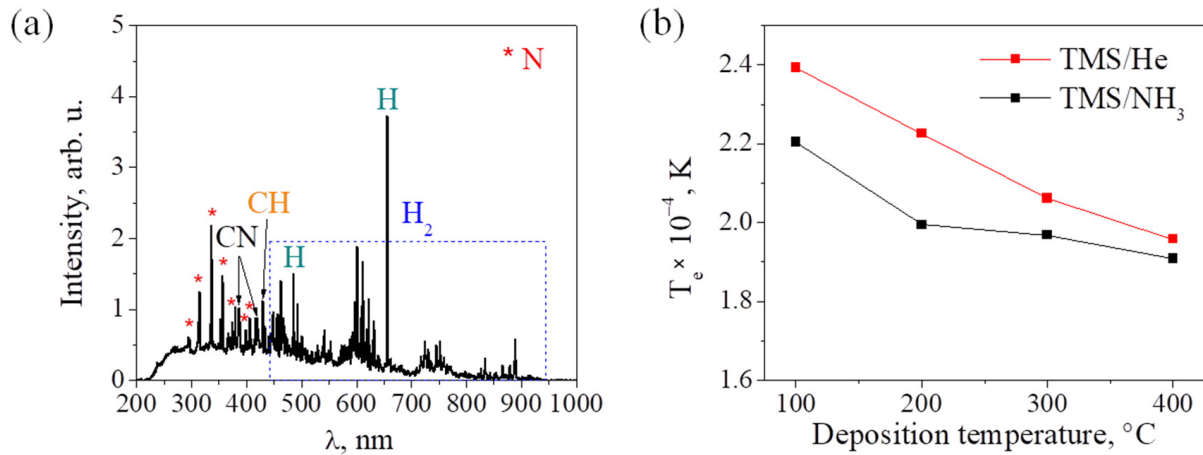


Figure 1. Emission spectrum of TMS plasma. N₂ bands were marked by asterisks (a); electron excitation temperature in TMS/He and TMS/NH₃ plasmas vs. deposition temperature (b).

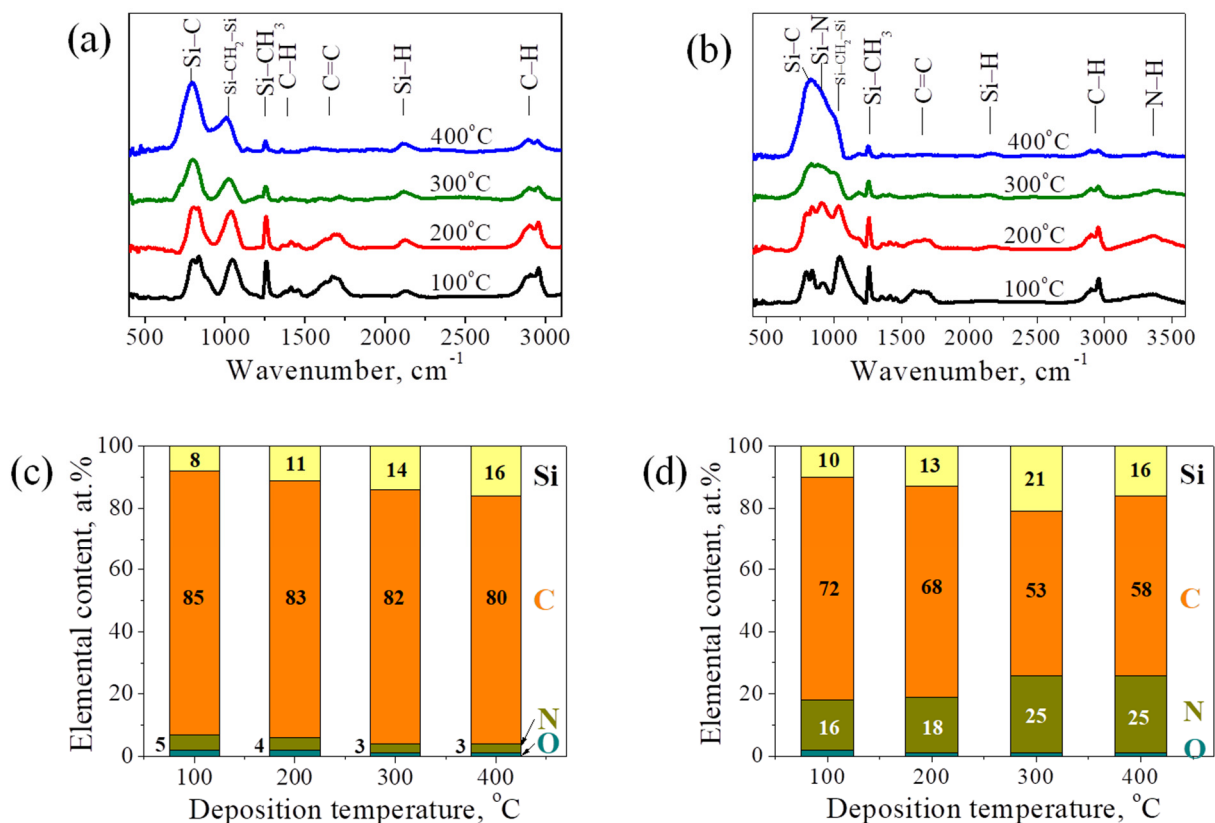


Figure 2. FTIR spectra (a,b) and EDX elemental composition (c,d) of SiC:H (SiCN:H) films deposited using TMS/He (a,c) and TMS/NH₃ (b,d) gas mixtures.

FTIR spectroscopy is the most widely used technique for determining the chemical bonding structure in SiCN:H films. This method has two important advantages over XPS. First, it allows for obtaining information about the character of the bonds presented in the bulk of the film. This is especially important for hydrogenated silicon carbonitride,

where the film surface often changes under environmental conditions and its composition and chemical bonding structure can differ significantly from the bulk. Second, FTIR spectroscopy makes it possible to describe the environment of atoms in terms of the presence of hydrogen atoms. However, correct assignment of FTIR signal to a certain group is a difficult task. In the review [24], we presented a table with literature data on values of the positions of absorption bands for various types of bonds presented in SiCN:H films. The values used in this work are given in Table 3 with references.

Table 3. FTIR absorptions.

Vibration	Band Position (in This Study), cm^{-1}	Band Position (Literature), cm^{-1}	Ref.
Si–C stretching	790	796–805	[41]
N–Si ₃ asymmetric stretching	840	850	[30]
Si–N stretching	920	911	[41]
Si–CH _x –Si wagging	1040	1020	[42]
Si–CH ₃ symmetric bending	1255	1260	[42]
C–H symmetric deformation	1354	1335–1390	[43]
C=C/C=N stretching	1650	1500 (C=C) 1600 (C=N)	[7]
SiH _n stretching ($n = 1-3$)	2110	2000–2100	[44]
C≡N	2200	2200	[42,45]
C–H stretching	2865	2896–2953	[41]
	2905		
	2956		
N–H stretching	3400	3382	[41]

The IR spectra of all films obtained under the conditions of a low-power plasma using helium as a plasma-forming gas (Figure 2a) contain absorption bands in the regions of 790 cm^{-1} , $1020-1040 \text{ cm}^{-1}$, $\sim 1600 \text{ cm}^{-1}$, corresponding to Si–C, Si–CH_x–Si, and C=C vibration modes, which indicates the polymerization of the precursor with a formation of silicon–carbon–silicon chains with incorporation of large hydrocarbon fragments. The intensity of Si–C signal increased with rise of deposition temperature. At the same time, a lowering of the intensity of bands related to C–H bond vibrations in the region of $2850-3000 \text{ cm}^{-1}$, $1350-1460 \text{ cm}^{-1}$, $\sim 1255 \text{ cm}^{-1}$, which indicates the destruction of hydrocarbon fragments with an increase in the synthesis temperature, accompanied by the following ejection of the corresponding gas species through the vacuum. The Si–H band relative intensity remains almost constant in the whole deposition temperature range. It is worth mentioning, that Si–H bond was not presented in the precursor molecule and was formed in the plasma conditions. It was also observed in several investigations [30,46].

It can be observed that FTIR spectra of the films deposited using TMS/NH₃ gas mixture have quite different features (Figure 2b). The N-containing absorption bands assigned to N–H (3400 cm^{-1}) and Si–N (920 cm^{-1}) stretching vibration modes appeared, pointing out that N atoms originated from ammonia molecule actively incorporated into the film. The relative intensity of the wide peak at $700-1200 \text{ cm}^{-1}$ rose, which can be due to increasing value of the crosslinking process. The peak is composed by a set of absorption bands defining preferential binding in the film. The signals attributed to Si–C, Si–N, Si–CH_x–Si/Si–O vibration modes can be observed. The contribution of Si–N component (920 cm^{-1}) rose with deposition temperature increasing, while Si–C absorption band remained intensive. The content of hydrogen-containing bonds decreased, leading to the material structuring by rearrangement accompanied by elimination of hydrogen-containing gas species. The intensity of the band assigned to Si–H vibration mode is negligible, which indicates the dominant role of Si–N bonds formation preventing Si–H binding.

The elemental composition of the films was evaluated using EDX analysis. It should be mentioned that the method is insensitive to hydrogen concentration; therefore, the information on presence of hydrogen atoms and tendencies of its concentration change can be estimated by FTIR analysis. The films contained silicon, carbon, nitrogen, and impurity of oxygen (less than 5 at.%) in the composition due to the result of EDX measurements. SiC:H films deposited using TMS/He gas mixture were carbon-rich in the whole deposition temperature range. The little admixture of nitrogen (5 at.% and less) was found, originating from residual pressure in the CVD camera. The concentration of silicon grew from 8 to 16 at.% along with the decrease in carbon content with the rise of deposition temperature that can be attributed to elimination of hydrocarbon groups, and is in a good assignment with FTIR data. The introduction of ammonia into reactive mixture led to the incorporation of N atoms into the film. The concentration of nitrogen in SiCN:H films increased from 16 to 25 at.% with the rise of deposition temperature from 100 to 400 °C. However, the use of the initial gas mixture with an excess of TMS, characterized by the ratio TMS/NH₃ = 2.5, led to the formation of the C-rich films. The ratio of C/Si in the SiC:H films exceeded the value C/Si = 4, corresponding to the TMS molecule in the whole range of synthesis temperature, which indicates the formation of aliphatic bridges in the SiC:H matrix.

The deposition rate was determined by the dividing of ellipsometric thickness to the synthesis time. The dependences of the growth rate on the deposition temperature for TMS/He and TMS/NH₃ initial gas mixtures are presented in Figure 3. The values of growth rate decreased with rise of deposition temperature from 33 to 20 nm/min for TMS/He mixture, and from 25 to 13 nm/min for TMS/NH₃ mixture. This tendency is typical for the PECVD process and was observed in different precursors [47–50]. Two main factors contribute to the tendency: the lowering of adsorption of film-forming precursors onto the growth surface with rise of deposition temperature, and the densification of the film due to the thermally induced elimination of organic moieties that is confirmed by FTIR and EDX data. This process is promoted by reduction of hydrogen-containing bonds and increasing of cross-linking level. The additional drop of growth rate in the case of TMS/NH₃ mixture can originate from two reasons: chemical reactions with formation of Si–N bonds accompanied by removal of –CH₃ fragments, and the bombardment of growing film by active NH₃ plasma species. The deposition rate corresponds or even exceeds the values presented in literature for TMS precursor, that was 6 nm/min in [27], 14–18 nm/min in [30], and 2–20 nm/min in [51].

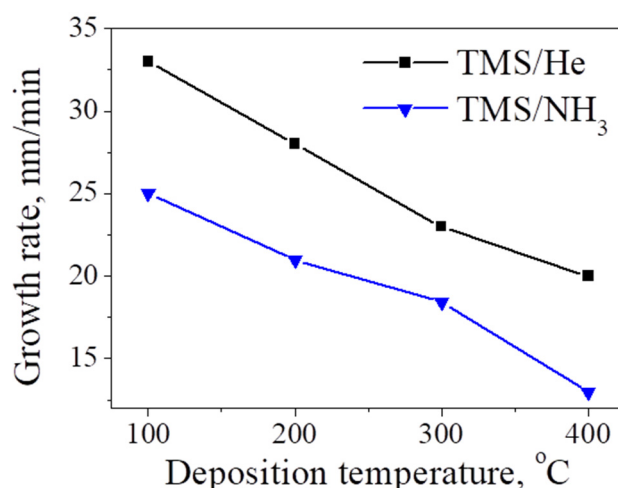


Figure 3. Deposition rate of SiC:H (SiCN:H) films deposited using TMS/He or TMS/NH₃ initial gas mixture as a function of deposition temperature.

Some optical properties of SiCH (SiCN:H) films, such as transmittance (Figure 4a,b), band gap (Figure 4c) and refractive index (Figure 4d) have been studied. The light transmittance measurements verify the optical quality of the films [52]. The transmission spectra

were recorded for test samples of SiC:H(SiCN:H)/SiO₂. The spectrum of bare fused silica is also presented in Figure 4a,b for comparison, its transmittance remains nearly constant at 93%–94% in the range of 500–1750 nm. The spectra of the samples exhibit characteristic sinusoidal interferences that depend on the thickness of the films, and the difference in refractive indices of the substrate and the film. The redshift of the transmittance spectra with an increase in deposition temperature is observed for both initial gas mixtures, and the most significant changes were detected for SiC:H samples. Two reasons could be regarded: intrinsic absorption due to the change of chemical composition, and reflection or interference effect. Based on literature data, long carbon chains of Si(CH₂)_x do not absorb visible and most of UV light [53]. The results of FTIR and EDX analysis showed that increase in deposition temperature led to the elimination of hydrocarbon fragments with formation of the films with SiC_x or SiC_xN_y composition. The comparison of the spectra for films deposited using TMS/He and TMS/NH₃ mixtures reveals that Si–N bonds used to be more effective for transparent layer creation, thus the transmission degradation is not so significant.

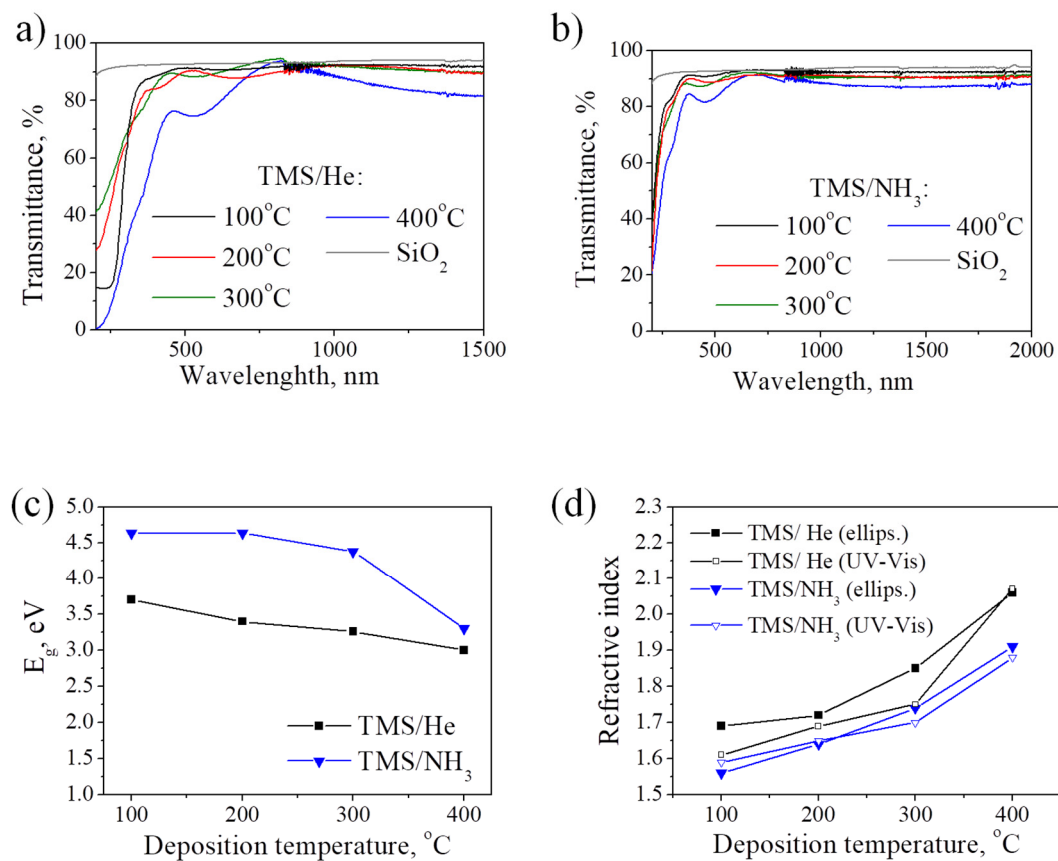


Figure 4. Optical properties of SiC:H (SiCN:H) films: evolution of transmittance of SiC:H/SiO₂ structures (a) and SiCN:H/SiO₂ structures (b), deposition temperature dependences of optical bandgap (c) and refractive index (d) obtained using UV-Vis and ellipsometry data.

The band gap was estimated using the results of a UV-Vis spectroscopy by Tauc's equation: $\alpha h\nu = B(h\nu - E_g)^n$, where α is the absorption coefficient, $h\nu$ is the incident photon energy, B is the dimensionless density of states constant and n is the parameter related to the density of states distribution [37]. The value of n was chosen as 2, that is characteristic for SiCN films [17]. The deposition temperature dependences of optical bandgap are presented in Figure 4c. Optical bandgap for SiC and Si₃N₄ are 3.3 and 5.4 eV, correspondingly [54]. These values are in agreement with the data obtained in this work. E_g values for SiC:H films deposited using TMS/He mixture were 2.8–3.7 eV. Ammonia addition into the reactive mixture led to the formation of SiCN:H films with optical bandgap of 3.6–4.6 eV. Thus, the

incorporation of nitrogen atoms into the film even up to 16–25 at.% with the formation of N–H and Si–N bonds made a significant contribution to the change of optical properties. For both SiC:H and SiCN:H films, a decrease in the values of E_g was observed with a rise of the synthesis temperature, which seems to be mainly associated with change of the chemical structure of the films from polymeric-like to ceramic-like.

The refractive index of the films was measured by laser ellipsometry at 632.8 nm. Deposition temperature dependence of refractive index is presented in Figure 4d. With an increase in the synthesis temperature, a rise of the refractive index was observed: from 1.68 to 1.96 for films deposited using a TMS/He mixture and from 1.56 to 1.90 for films obtained using a TMS/NH₃ mixture. Regarding the Lorentz–Lorenz correlation, an increase in the refractive index can be associated with both an increase in the film density and a change in the chemical composition that affects the polarization response of the material [2,55]. The trend of CVD films densification with deposition temperature increasing and its relation with refractive index was studied in detail for different organosilicon precursors by Prof. Wrobel's group [17]. On the other hand, SiCN:H films deposited using a TMS/NH₃ gas mixture are characterized by elevated concentrations of N atoms and presence of Si–N bonds that decrease in n values in comparison to SiC:H films produced using TMS/He mixture. To control the consistency of ellipsometrical and UV-Vis data, refractive index values were estimated from transmission spectra, according to the method given in [56] (Figure 4d). A similarity of the trends in the change of refractive index with increasing deposition temperature is observed. A certain difference in the values of n obtained from ellipsometry and UV-Vis data may be attributed to some non-uniformity in thickness of the films, as well as the lack of expression of the maxima in the spectra.

3.2. Variation of NH₃ Concentration in Initial Gas Mixture

The effect of ammonia concentration in the initial gas mixture on the composition, chemical binding structure and optical properties of the films was studied for the samples at 400 °C. The total pressure of the initial gas mixture was the same in order to save the characteristics of plasma, but the ratio NH₃/TMS was changed from 0 to 2.5.

The FTIR and EDX data are presented in Figure 5. It should be noted that an increase in the ammonia concentration led to a significant change in both the character of FTIR spectra and elemental composition. Even a small addition of NH₃ at NH₃/TMS = 0.4 into a gas mixture resulted in a strong incorporation of nitrogen atoms into the film up to 25 at.% accompanied by formation of Si–N (920 cm⁻¹) and N–H (3400 cm⁻¹). The absorption bands of C–H bonds (~2800 cm⁻¹, 1255 cm⁻¹, 1020 cm⁻¹) were maintained. The further increase in ammonia concentration up to NH₃/TMS = 1 resulted in silicon nitride formation. The wide absorption band in fingerprint region of 750–1050 cm⁻¹ narrowed, the single maximum at 870 cm⁻¹ was observed assigned to a combination of Si–N (920 cm⁻¹) and N–Si₃ (840 cm⁻¹) bonds [5,30]. The bands assigned to Si–H and N–H bonds were also presented, while hydrocarbon groups' signals were not detected. The elemental composition of the films also changed. The main elements were silicon and nitrogen, while oxygen and carbon were registered at the level of 2 at.%. The further enrichment of the gas phase with ammonia did not change the character of FTIR spectra and elemental composition significantly. Thus, the use of the gas mixture with equal content of TMS and NH₃ is enough to produce SiN:H films at 400 °C. It is worth mentioning that this is a feature for a low-power process, when the precursor does not decompose completely to the single atoms in the plasma conditions. The use of high plasma power of 1500 W led to the formation of SiCN films with an excess of carbon even at [TMS]/[NH₃] = 0.5 [30]. The films produced by MWPECVD at total plasma power of 1000 W at TMS/NH₃ = 0.68 were close to SiC_x and were characterized by a composition of Si_{0.36}C_{0.55}N_{0.08}O_{0.01} [5].

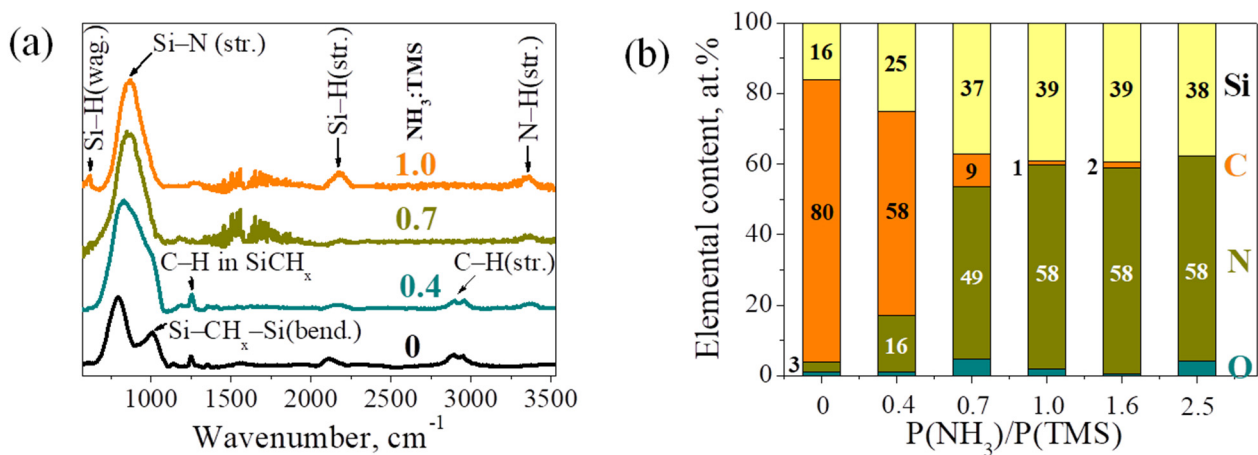


Figure 5. FTIR spectra (a) and EDX elemental composition (b) of SiC:H (SiCN:H) films deposited using TMS/NH₃ gas mixture at 400 °C.

The curve of deposition rate change with a rise in ammonia concentration in the initial gas mixture is presented in Figure 6. A drop in growth rate from 20 nm/min to 5 nm/min with NH₃/TMS ratio increasing from 0 to 1 is observed. Then, during further enrichment of gas mixture by ammonia, the value decreased slightly to 2 nm/min. The significant factor defining such behavior is the decrease in the TMS concentration. As a source of silicon and carbon, it is the most significant compound for film creation. The second reason is treatment of hydrocarbon species from the film during bombardment of the growing film by active species, produced in ammonia plasma. This is an important process influenced the deposition rate, as the drop of deposition rate stopped when the film composition was close to SiN:H.

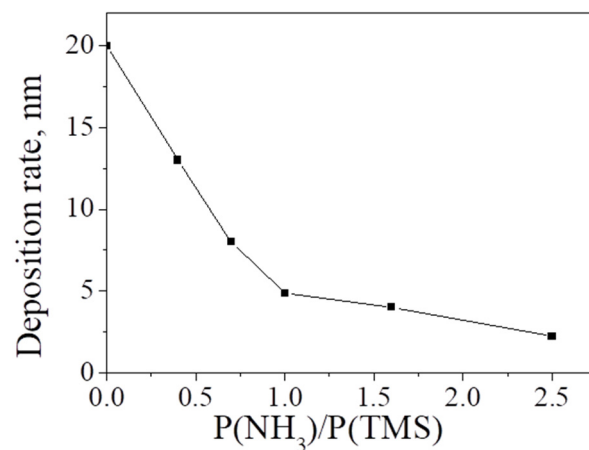


Figure 6. Deposition rate of SiC:H (SiCN:H) films deposited at 400 °C using various compositions of TMS/NH₃ initial gas mixture.

Evolution of transmittance, optical bandgap, and refractive index with change of initial gas mixture is presented in Figure 7. The blueshift of transmission coefficient was observed with an increase in ammonia concentration. The related parameter of optical bandgap demonstrated a stepwise increase from 3.3 eV to 5.0 eV at NH₃/TMS = 0.6. Such a behavior was observed previously in several publications for SiCN films produced using different precursors [14,57–59]. The main reason can be a change of chemical binding structure. The films produced using ammonia-rich initial gas mixture are characterized by a higher N/Si ratio and higher relative concentration of Si–N bond in FTIR spectra, thus their bandgap increases. The value of 5.1 eV is typical for SiN_x films [60], which confirms the similarity of the produced films to silicon nitride. Moreover, the contribution of Si–H absorption band

increased, that additionally improved the bandgap [52]. The results can be compared with the data presented in the literature for films produced using TMS as a precursor. For SiCN films obtained from a TMS/N₂ mixture under the conditions of ICP CVD experiments [6], the band gap was 2.7–3.6 eV. The nitrogen content in the films varied within a narrow range of 10–20 at.%. Thus, the use of ammonia as an additional gas seems to be a more efficient method for varying the composition and properties of films. In [61], the nitrogen content in the films was varied by introducing 1% hexamethyldisilazane into the TMS flow. The nitrogen content in the films was approx. 1 at.%, the band gap varied in the range of 2.3–2.7 eV. SiCH:Cl films were obtained from a mixture of TMS and chloroform. It is shown that the band gap varies in the range of 2.4–3.5 eV with an increase in the chlorine content in the film up to 4 at.% [62]. The presented set of data show that by varying the synthesis conditions, using TMS as the precursor, it is possible to obtain films with the band gap ranged in a wide area.

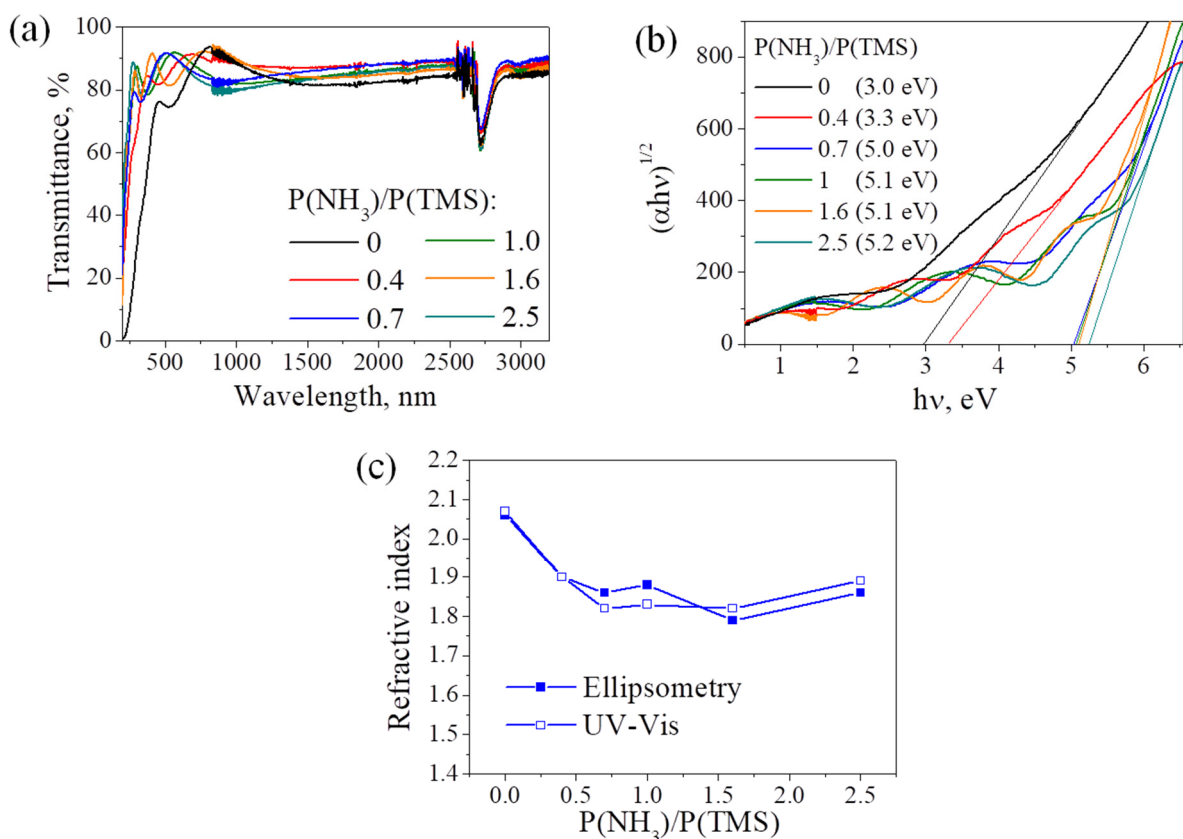


Figure 7. Optical properties of SiC:H (SiCN:H) films: evolution of transmittance of SiCN:H/SiO₂ structures (a), optical bandgap (b), and refractive index (c), with variation of gas ratio in the initial mixture of NH₃/TMS.

Figure 7c shows the refractive index for various ratios of NH₃/TMS obtained by ellipsometry and estimated using UV-Vis data. Refractive index was 2.1 for SiCN film deposited using TMS/He mixture, and decreased to 1.78–1.90 with the introduction of ammonia into the reactive mixture. The discussed previous dependence of n values on the chemical composition seems to have a leading contribution. The appearance of Si–N bonds at NH₃/TMS = 0.4 and increasing of its concentration, which was confirmed by FTIR, decreased refractive index crucially. The relationship between Si–C concentration in the films and their refractive index was previously discussed in details in [29,63].

3.3. Surface Modification by He, O₂, NH₃ Plasma

The sample deposited using the initial gas mixture ascribed by P(NH₃)/P(TMS) = 0.4 at 400 °C with a thickness of 200 nm was chosen for wettability characterization. PECVD SiCN:H films possess reduced hydrophilic or even hydrophobic with average water contact angle (CA), ranging from 56 to 105° depending on deposition technique, and synthesis conditions [46,64,65]. This makes them suitable for biomedical applications, where it helps to prevent protein adsorption and the lubricity of the urinary catheters, as well as material creation, as a sublayer to achieve a good adhesion between the coating and the substrate [66–68]. In this work we applied an approach of surface modification by plasma treatment which is often used to improve the hydrophilic properties of polymers [69,70], and also for modification of low-k materials to reduce bulk damage [71]. The SiCN:H sample was exposed in the atmosphere of He, O₂ or NH₃ plasma for 5 min. Figure 8a presents the values of CA for the initial and plasma treated surfaces, obtained for water and diethylene glycol test liquids. The tendencies of CA changing are similar for both substances, the water contact angle (WCA) evolution will be considered below. The value of WCA was equal to 71° for the initial sample, which may be regarded as slightly hydrophilic film. This result is in consideration with the WCA data presented in literature for SiCN:H films deposited using different precursors: for tetramethyldisilazane it varied in the range of 62–78° [45], hexamethyldisilazane—78–83° [72], and bis(dimethylamino)dimethylsilane—56–78° [46]. The plasma treatment of the sample resulted in a drastic decrease in WCA to 36–42°. The values differed slightly with a change of gas type (Figure 8a).

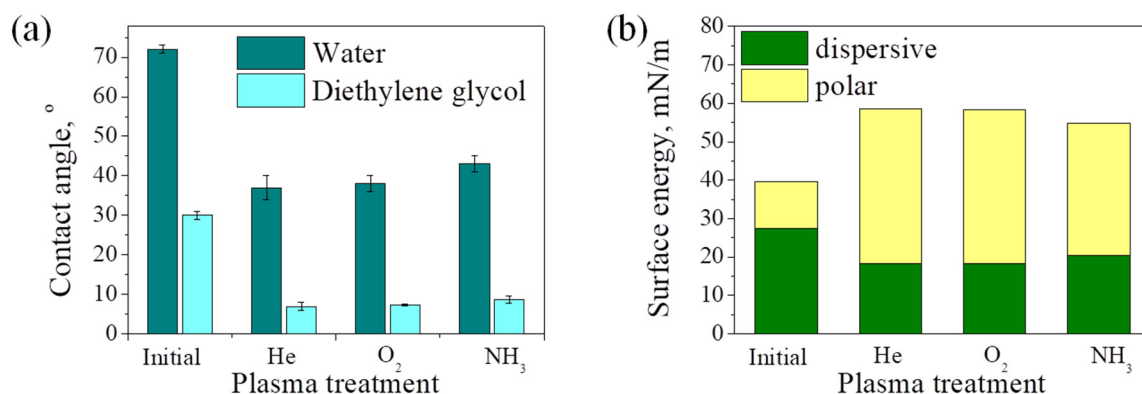


Figure 8. Behavior of the contact angle (water and diethylene glycol) (a) and surface energy (b) in dependence on plasma treatment chemistry.

The main factors influencing wettability of the coating are surface energy and surface roughness. The values of CA obtained for water and diethylene glycol test liquids were used for calculation of surface free energy, the results are presented in Table 4. The contribution of dispersive and polar components is demonstrated in Figure 8b. A non-treated sample possessed a relatively low total surface energy with a small contribution of polar energy parts. After plasma processing a strong increase in the polar part was observed, while the dispersive part slightly decreased. The rise of the polar component seems to be a result of chemical bonding structure change, attributed to the presence of an increased number of terminal groups.

The chemical bonding structure of the films was studied by FTIR analysis and XPS. The treatment of the films by plasma resulted in strong changes in FTIR spectra (Figure 9a). The main difference between the initial film and the films treated with all gases concerned hydrogen-containing bonds. The absorption bands related to hydrocarbon fragments: Si–CH_x–Si (1020 cm^{−1}), Si–CH₃ (1260 cm^{−1}), C–H (2800–3000 cm^{−1}), and also Si–H (2120 cm^{−1}) bonds, that are characteristic for the initial film, completely disappeared after processing. As the depth of IR analysis exceeds the film thickness, the result showed that the bulk part of film underwent rearrangement during the treatment accompanied by

dehydrogenization. The main broad absorption band at 500–700 cm^{-1} also changed. The position of its maximum was 800 cm^{-1} for the initial film, which corresponds to the Si–C bond. Processing of the film in the plasma of inert helium and oxygen led to a shift of the maximum to 840 cm^{-1} , which is an intermediate value between the Si–C and Si–N positions, and also the N–Si₃ fragment [5]. After treatment in ammonia plasma, the absorption band assigned to Si–N became the dominant component. It is interesting to note that the spectrum of the film treated in oxygen plasma did not contain an additional absorption band corresponding to the Si–O bond. Thus, it seems that the Si–O layer formed on the surface impeded the consequence oxidation of the film [73].

Table 4. Evolution of the surface characteristics of SiCN films after exposure in He, O₂ or NH₃ plasma.

Plasma Treatment	WCA, °	Free Surface Energy, mN/m (Neumann/Owens–Wendt/Wu)	RMS, nm	XPS and FTIR Bonding Structure, Main Bonds
Initial	71	40.2/39.6/43.2	1.63	Si–C, C–H (less Si–N)
He	36	54.3/58.6/62.3	0.67	Si–O, Si–C, Si–N
O ₂	37	54.1/58.4/62.0	0.63	Si–O, (less Si–C, Si–N)
NH ₃	42	52.1/54.8/59.0	0.71	Si–N, Si–C, C–N/C=N

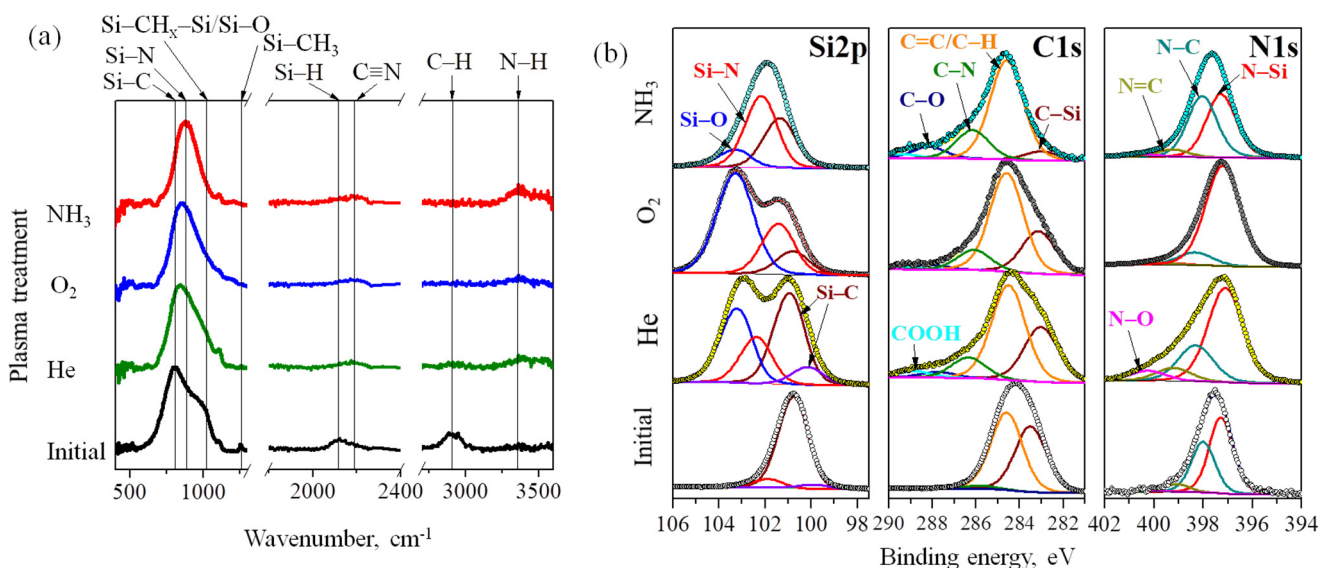


Figure 9. FTIR (a) and XPS (b) Si2p, C1s, N1s core-level spectra of initial SiCN film and after He, O₂ or NH₃ plasma treatment in helium, oxygen, and ammonia.

The change of surface chemistry after the treatment was examined by XPS. Si2p, C1s and N1s core-level spectra are presented in Figure 9b. The spectra interpretation was performed using the literature data [16,41,74,75]. The Si2p spectrum was fitted with four components at 99.8–100.1, 100.9–101.3, 101.2–102.3, and 103.2–103.3 eV, that can be attributed to Si–C as a part of the Si–C–Si environment in stoichiometric SiC, Si–C in the fragment where some atoms are substituted with N or O [76], Si–N, and Si–O bonds, correspondingly. C1s spectrum was resolved to five+ components at 283.02–283.5, 284.6, 286.1, 287.5–288.1, 288.8–289.4 eV assigned to C–Si, C–C/C–H, C–N, C=O, C–COOH, correspondingly. For N1s peak, four main components can be distinguished in the regions of about 397.1–397.3, 398.0–398.3, 399.1–399.3 eV, 400.0–400.4 eV corresponding to the N–Si, N–C, N=C, and N–O bonds.

The Si2p spectrum of the initial sample mainly consists of Si–C components with a low concentration of Si–N, which is consistent with FTIR results. A slight contribution of N–Si and N–C/N=C bonds is observed in N1s spectrum.

The treatment in He plasma resulted in a decrease in Si–C peak in the Si2p spectrum due to hydrocarbon fragments elimination by the bombardment of the surface by active plasma species, that is in agreement with FTIR data. The relative intensity of Si–O exceeded Si–N, which can be explained by a surface oxidized layer, since XPS is a surface sensitive method. It is proved by the presence of oxidized bonds of C–O and COOH in C1s spectrum. The rearrangement provided by modification in He plasma also concerned carbon to nitrogen bonds that were expressed in the growth of N–C/N=C and nitrile contributions in the N1s spectrum, and the C–N component in the C1s spectrum.

Si2p spectrum of the sample treated in oxygen plasma can be resolved in two components related to Si–C and Si–O bonds, thus the surface of the film is close to SiO₂. Concurrently, N atoms are presented in the environment of Si that is pointed out by the position of the Si–C peak at 101.3 eV. As FTIR analysis showed an absence of Si–O bonds in the bulk of the material, it can be proposed that the oxidation affected only the surface. The layer of SiO₂ seems to hinder the following diffusion to the deeper layers, considering the low temperature of the process.

The processing in NH₃ plasma changed the spectra significantly. Relative intensity of Si–N in the Si2p component grew with the serve of the Si–C peak. On the other hand, the concentration of CN also increased, which is depicted by the presence of strong contributions of C–N in C1s peak and N=C, N–C in N1s peak, making the top layer of the film close to SiCN, which contained bonds between all of the elements involved. Less oxidation than in the case of He treatment can be associated with passivation of the surface with nitrogen, which makes it difficult to oxidize the surface of the sample when it is removed from the reactor into air.

The study of the films by FTIR spectroscopy and XPS made it possible to obtain the most complete information about the character of the bonds presented in the films. The XPS method helped clarify the environment of the Si, C, and N atoms, while the FTIR analysis provided information on the types of the hydrogen-containing bonds. There is agreement between the XPS and FTIR data with respect to the dominant bonds in the films. The chemical bonding structure of the untreated film was described in Section 3.1. Comparison of FTIR and XPS data for the initial SiCN:H film confirmed that the main bond was Si–C. The XPS data made it possible to supplement the information on the environment of nitrogen atoms. It was shown that there is a small concentration of the Si–N bond, as well as various nitrogen to carbon bonds. In addition, the films involved hydrogen-containing bonds of Si–CH_x–Si, Si–H, C–H, N–H. According to FTIR spectroscopy, the initial SiCN film was the most hydrogenated, and its treatment in plasma in all cases led to a significant decrease in the intensity of these components. During treatment in He plasma, probably due to the predominant etching of carbon atoms, an increase in the relative contribution of the Si–N and Si–O bonds was observed, which was shown by FTIR and XPS. The position of the main peak in the FTIR spectrum shifted to an intermediate position between Si–C and Si–N, and a peak asymmetry was observed, indicating the presence of the Si–O component. The XPS method showed the presence of the various carbon to nitrogen bonds, while the corresponding absorption bands were not observed in the IR spectrum. This may indicate the formation of these fragments on the surface upon treatment with helium plasma. The study of the sample treated in oxygen plasma showed the greatest difference in the results of FTIR and XPS. According to the XPS data, characterizing the film surface, the dominant bond was Si–O, which indicated the oxidation of the sample. However, the FTIR spectra of the films contained only the Si–O shoulder, and the position of the maximum of the main peak was intermediate between Si–C and Si–N. It seems that the Si–O layer formed on the surface impeded the consequence of oxidation of the film. As a result of treatment of the SiCN film in ammonia plasma, Si–N became the main bond, which was confirmed by FTIR and XPS data; however, Si–C and Si–O bonds were also present. C–N bonds were also formed on the film surface as a result of deeper nitridization, but they were not detected in the bulk of the film. Thus, we can conclude that the treatment of the SiCN:H film in plasma affected the entire volume of the film, which was expressed in a change in the dominant

bond, as well as in dehydrogenization of the films. However, the surface underwent more serious changes that proceeded with the formation of nitride and silicon oxide, as well as the formation of C–N bonds. Regarding the relationship between wettability and chemical bonding structure of the film surface, slightly hydrophilic properties of the initial SiCN:H film are mostly likely due to the presence of a combination of hydrophobic terminal non-polar C–H and Si–H and hydrophilic N–H and Si–O chemical bonds. The wettability of the film increased after plasma treatment. An important role in this process is played by the complete disappearance of C–H groups. Since the Si–C component in the Si2p XPS spectrum reduced significantly, it can be assumed that the elimination of hydrophobic methyl groups took place. The similar correlations were obtained in [77] for PECVD SiCN:H films deposited from hexamethyldisilazane at different deposition temperatures. After treatment in helium or oxygen plasma, the hydrophilic properties of the films increased, that is associated with appearance of hydrophilic bonds. The broken Si–C bond may form into Si–O, C–O or Si and C dangling bonds [78]. Si–O bond formation is most likely due to the polymerization of silanol bonds that could occur at even room temperature if the two OH groups were close neighbors, such as those with hydrogen [79]. The creation of Si–O bonds after treatment in inert Ar plasma was also observed in [80]. The authors explained it by the easy oxidation of damaged SiCN film. The XPS data confirmed the oxidation of surface layer with the formation of Si–O, COOH, C–O, N–O bonds. OES data presented in Figure 1 pointed the residual air in the vacuum system that could promote formation of oxidized states. On the other hand, it is well known from this that plasma polymers are very rich in radicals [81], which can be a source of additional Si–O bonds formed when exposed to the ambient conditions. N–H groups, observed by FTIR analysis of the SiCN:H sample treated by NH₃ plasma, are less polar than oxygen-containing bonds, which explains lower wettability of the samples in comparison with O₂ and He treatment.

In order to estimate the contribution of surface morphology to the wettability of the films, the roughness of the films was examined by AFM. The typical AFM planar view is presented in Figure 10. The samples had a smooth and homogeneous surface. The RMS of the untreated sample was 1.6 nm. The processing in the plasma led to the smoothing of the surface to the RMS values of 0.6–0.7 nm. Such a behavior can be attributed to the elimination of the hydrocarbon species that was demonstrated by FTIR analysis, and the following rearrangement with the formation of dense structure.

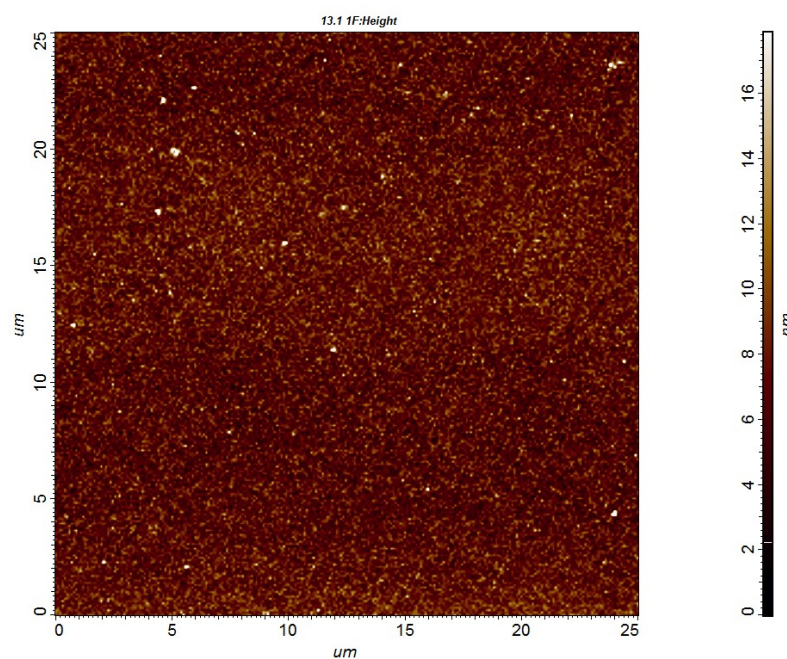


Figure 10. Typical AFM image of SiCN sample.

All the modifications that occurred with the SiCN sample during the treatment in different plasma are summarized in Table 4. It can be concluded that the main changes in wettability are determined by the type of the bonds presented on the surface of the sample. The most significant change in the structure of the films after all types of treatment was the loss of hydrogen. Non-polar hydrogen-containing bonds can increase the hydrophobicity of the material, and their exclusion led to a drop in the values of the WCA. The other factor that slightly affected the wettability of the treated samples was the change of concentration of silicon-containing bonds. The polarity of them decreases in the row: Si–O > Si–N > Si–C. XPS analysis showed that the treatment with ammonia leads to the formation of a surface layer containing Si–C and Si–N bonds at a relatively low content of Si–O. Processing of the film in an oxygen and helium plasma led to a significant increase in the concentration of the more polar Si–O bond. The presence of residual oxygen in the reactor led to the oxidation of the film even in the plasma of inert helium. Thus, an increase in wettability was observed in the row: initial—NH₃—O₂~He. The change in roughness observed for the plasma-treated samples probably did not have a significant effect on the wettability of the samples due to small changes.

4. Conclusions

PECVD SiC(N):H films with nitrogen concentration changed in a wide range were produced using TMS and helium (or ammonia) mixture. Use of low-power RF plasma led to partial fragmentation of the precursor molecule with preservation of Si–C bonds that resulted in formation of the films with predominant binding between silicon and carbon. However, the chemical bonding structure and composition of the films are shown to be sensitive to ammonia concentration in the reactive mixture. The transition from SiCN:H to SiN_x:H film occurred at the ratio of NH₃/TMS equal to 1. The investigation showed the ability to produce films of highly variable optical properties by change the deposition conditions. The growth of refractive index and lowering of bandgap in the range of 1.55–2.05 and 4.06–3.0 eV, correspondingly, was observed with increase in deposition temperature. Introduction of excess of ammonia into the initial gas phase allowed enlarging the bandgap up to 5.2 eV.

Surface modification by plasma treatment is often used to improve the hydrophilic properties of organic polymers. In this work, SiCN:H film was modified by processing of SiCN film in the various type of plasma (He, O₂, NH₃). The plasma treatment of SiCN:H film changed its wettability from slightly hydrophilic (WCA = 71°) to hydrophilic (36–42°), thus it increased in the row: untreated < NH₃ treatment < O₂ treatment~He treatment. The analysis of surface free energy revealed the significant variation in its polar component, pointing out the chemical bonding structure change, attributed to the presence of an increased number of terminal groups. XPS and FTIR investigations showed that not only the surface, but bulk of the film underwent significant changes. Hydrogen-containing fragments were eliminated from the whole volume of film, which was shown by FTIR analysis of treated samples. The additional changes concerning Si, C and N atoms were observed by XPS analysis. Processing in oxygen plasma led to an increase in relative content of Si–O bonds, while NH₃ plasma treatment resulted in the formation of the SiCN surface layer, which included Si–C, Si–N, C–N and C=N bonds.

Author Contributions: Conceptualization, E.E. and M.K.; methodology, E.E. and M.K.; formal analysis, A.K., A.F., I.Y., V.S. and E.M.; investigation—E.E., M.K. and A.F.; writing—original draft preparation, E.E.; editing, M.K.; supervision, M.K.; project administration, M.K. All authors contributed to the discussion and interpretation of the results. All authors have read and agreed to the published version of the manuscript.

Funding: The research was supported by the Ministry of Science and Higher Education of the Russian Federation, project N 121031700314-5.

Institutional Review Board Statement: Not applicable.

Informed Consent Statement: Not applicable.

Data Availability Statement: Not applicable.

Acknowledgments: The authors thank A.A. Shapovalova, for the FTIR spectroscopy characterization.

Conflicts of Interest: The authors declare no conflict of interest.

References

1. Sha, B.; Lukianov, A.N.; Dusheiko, M.G.; Lozinskii, V.B.; Klyui, A.N.; Korbutyak, D.V.; Pritchins, S.E.; Klyui, N.I. Carbon-rich amorphous silicon carbide and silicon carbonitride films for silicon-based photoelectric devices and optical elements: Application from UV to mid-IR spectral range. *Opt. Mater.* **2020**, *106*, 109959. [[CrossRef](#)]
2. Khatami, Z.; Bleczewski, L.; Neville, J.J.; Mascher, P. X-ray Absorption Spectroscopy of Silicon Carbide Thin Films Improved by Nitrogen for All-Silicon Solar Cells. *ECS J. Solid State Sci. Technol.* **2020**, *9*, 083002. [[CrossRef](#)]
3. Khatami, Z.; Nowikow, C.; Wojcik, J.; Mascher, P. Annealing of silicon carbonitride nanostructured thin films: Interdependency of hydrogen content, optical, and structural properties. *J. Mater. Sci.* **2018**, *53*, 1497–1513. [[CrossRef](#)]
4. Chou, T.H.; Kuo, T.W.; Lin, C.Y.; Lai, F.S. A low cost n-SiCN/p-PS/p-Si heterojunction for high temperature ultraviolet detecting applications. *Sens. Actuators A Phys.* **2018**, *279*, 462–466. [[CrossRef](#)]
5. Plujat, B.; Glénat, H.; Hamon, J.; Gazal, Y.; Goullet, A.; Hernandez, E.; Quiozola, S.; Thomas, L. Near-field scanning microscopy and physico-chemical analysis versus time of SiCN:H thin films grown in Ar/NH₃/TMS gas mixture using MW-Plasma CVD at 400 °C. *Plasma Process. Polym.* **2018**, *15*, 1800066. [[CrossRef](#)]
6. Rumyantsev, Y.M.; Chagin, M.N.; Shayapov, V.R.; Yushina, I.V.; Kichai, V.N.; Kosinova, M.L. Synthesis and Properties of Thin Films Formed by Vapor Deposition from Tetramethylsilane in a Radio-Frequency Inductively Coupled Plasma Discharge. *Glass Phys. Chem.* **2018**, *44*, 174–182. [[CrossRef](#)]
7. Zhuang, C.; Schlemper, C.; Fuchs, R.; Zhang, L.; Huang, N.; Vogel, M.; Staedler, T.; Jiang, X. Mechanical behavior related to various bonding states in amorphous Si–C–N hard films. *Surf. Coat. Technol.* **2014**, *258*, 353. [[CrossRef](#)]
8. Fainer, N.I.; Kosinova, M.L.; Rumyantsev, Y.M.; Maximovskii, E.A.; Kuznetsov, F.A. Thin silicon carbonitride films are perspective low-k materials. *J. Phys. Chem. Solids* **2008**, *69*, 661. [[CrossRef](#)]
9. Szymanowski, H.; Olesko, K.; Kowalski, J.; Fijalkowski, M.; Gazicki-Lipman, M.; Sobczyk-Guzenda, A. Thin SiNC/SiOC Coatings with a Gradient of Refractive Index Deposited from Organosilicon Precursor. *Coatings* **2020**, *10*, 794. [[CrossRef](#)]
10. Wrobel, A.M.; Blaszczyk-Lezak, I. Remote Hydrogen Microwave Plasma CVD of Silicon Carbonitride Films from a Tetramethylsilazane Source. Part 2: Compositional and Structural Dependencies of Film Properties. *Chem. Vap. Depos.* **2007**, *13*, 595–600. [[CrossRef](#)]
11. Guruvenket, S.; Andrie, S.; Simon, M.; Johnson, K.W.; Sailer, R.A. Atmospheric-Pressure Plasma-Enhanced Chemical Vapor Deposition of a-SiCN:H Films: Role of Precursors on the Film Growth and Properties. *Appl. Mater. Interfaces* **2012**, *4*, 5293–5299. [[CrossRef](#)] [[PubMed](#)]
12. Fainer, N.I. From organosilicon precursors to multifunctional silicon carbonitride. *Russ. J. Gen. Chem.* **2012**, *82*, 43–52. [[CrossRef](#)]
13. Ermakova, E.; Lis, A.; Kosinova, M.; Rumyantsev, Y.; Maximovskii, E.; Rakhlin, V. Bis(trimethylsilyl)ethylamine: Synthesis, properties and its use as CVD precursor. *Phys. Proc.* **2013**, *46*, 209–218. [[CrossRef](#)]
14. Ermakova, E.; Mogilnikov, K.; Asanov, I.; Fedorenko, A.; Yushina, I.; Kichay, V.; Maksimovskiy, E.; Kosinova, M. Chemical Structure, Optical and Dielectric Properties of PECVD SiCN Films Obtained from Novel Precursor. *Coatings* **2022**, *12*, 1767. [[CrossRef](#)]
15. Cheng, Y.-L.; Lin, Y.-L. Comparison of SiC_xN_y barriers using different deposition precursors capped on porous low-dielectric-constant SiOCH dielectric film. *Thin Solid Films* **2020**, *702*, 137983. [[CrossRef](#)]
16. Ma, X.; Xu, C.; Mao, Z.; Ji, P.; Jin, C.; Xu, D.; Ding, Y. Synthesis, characterization, and thermal properties of novel silicon 1,1,3,3-tetramethylguanidinate derivatives and use as single-source chemical vapor deposition precursors. *Appl. Organomet. Chem.* **2020**, *34*, e5349. [[CrossRef](#)]
17. Wrobel, A.M.; Uznanski, P. Hard silicon carbonitride thin-film coatings by remote hydrogen plasma chemical vapor deposition using aminosilane and silazane precursors. 2: Physical, optical, and mechanical properties of deposited films. *Plasma Process. Polym.* **2021**, *18*, 2000241. [[CrossRef](#)]
18. Ng, Y.M.; Ong, C.W.; Zhao, X.A.; Choy, C.L. Polymerization of dual ion beam deposited CN_x films with increasing N content. *Vacuum Sci. Technol.* **1999**, *17*, 584. [[CrossRef](#)]
19. Fainer, N.I.; Plekhanov, A.G.; Golubenko, A.N.; Rumyantsev, Y.M.; Rakhlin, V.I.; Maximovski, E.A.; Shayapov, V.R. PECVD Synthesis of Silicon Carbonitride Layers Using Methyltris(diethylamino)silane as the New Single-Source Precursor. *J. Solid State Sci. Technol.* **2015**, *4*, N3153. [[CrossRef](#)]
20. Fainer, N.I.; Golubenko, A.N.; Rumyantsev, Y.M.; Kesler, V.G.; Ayupov, B.M.; Rakhlin, V.I.; Voronkov, M.G. Tris(diethylamino)silane—A new precursor compound for obtaining layers of silicon carbonitride. *Glass Phys. Chem.* **2012**, *38*, 15. [[CrossRef](#)]
21. Wrobel, A.M.; Blaszczyk-Lezak, I.; Uznanski, P.; Glebocki, B. Remote Hydrogen Microwave Plasma Chemical Vapor Deposition of Amorphous Silicon Carbonitride (a-SiCN) Coatings Derived from Tris (dimethylamino) Silane. *Plasma Process. Polym.* **2011**, *8*, 542. [[CrossRef](#)]

22. Zhou, Y.; Probst, D.; Thissen, A.; Kroke, E.; Riedel, R.; Hauser, R.; Hoche, H.; Broszeit, E.; Kroll, P.; Stafast, H. Hard silicon carbonitride films obtained by RF-plasma-enhanced chemical vapour deposition using the single-source precursor bis(trimethylsilyl)carbodiimide. *J. Eur. Ceram. Soc.* **2006**, *26*, 1325–1335. [CrossRef]
23. Smirnova, T.P.; Badalyan, A.M.; Yakovkina, L.V.; Sysoeva, N.H.; Asanov, I.P.; Kaichev, V.V.; Bukhtiarov, V.I.; Shmakov, A.N. Silicon carbonitride films synthesized from new sources. *Chem. Sustain. Dev.* **2001**, *9*, 23–29.
24. Ermakova, E.; Kosinova, M. Organosilicon compounds as single-source precursors for SiCN films production. *J. Organomet. Chem.* **2022**, *958*, 122183. [CrossRef]
25. Beake, B.D.; McMaster, S.J.; Liskiewicz, T.W. Contact size effects on the friction and wear of amorphous carbon films. *Appl. Surf. Sci. Adv.* **2022**, *9*, 100248. [CrossRef]
26. Maruno, H.; Nishimoto, A. Adhesion and durability of multi-interlayered diamond-like carbon films deposited on aluminum alloy. *Surf. Coat. Technol.* **2018**, *354*, 134–144. [CrossRef]
27. Nishikawa, J.; Sugihara, N.; Nakano, M.; Hieda, J.; Ohtake, N.; Akasaka, H. Effect of Si incorporation on corrosion resistance of hydrogenated amorphous carbon film. *Diamond Relat. Mater.* **2018**, *90*, 207–213. [CrossRef]
28. Wu, H.Y.; Hsu, C.H.; Liu, T.X.; Ou, Y.C.; Hsu, Y.H.; Wu, W.Y.; Lien, S.Y.; Jiang, Y.L. Silicon nitride cover layer prepared by silane-free plasma chemical vapor deposition for high quality surface passivation of silicon solar cells. *Surf. Coat. Technol.* **2019**, *376*, 68–73. [CrossRef]
29. Plujat, B.; Glénat, H.; Bousquet, A.; Frézet, L.; Hamon, J.; Goulet, A.; Tomasella, E.; Hernandez, E.; Quoizola, S.; Thomas, L. SiCN:H thin films deposited by MW-PECVD with liquid organosilicon precursor: Gas ratio influence versus properties of the deposits. *Plasma Process. Polym.* **2020**, *17*, 1900138. [CrossRef]
30. Silva, J.A.; Quoizola, S.; Hernandez, E.; Thomas, L.; Massines, F. Silicon carbon nitride films as passivation and antireflective coatings for silicon solar cells. *Surf. Coat. Technol.* **2014**, *242*, 157–163. [CrossRef]
31. Soum-Glaude, A.; Bousquet, I.; Thomas, L.; Flamant, G. Optical modeling of multilayered coatings based on SiC(N)H materials for their potential use as high-temperature solar selective absorbers. *Sol. Energy Mater. Sol. Cells* **2013**, *117*, 315–323. [CrossRef]
32. Chen, S.-W.; Wang, Y.-S.; Hu, S.-Y.; Lee, W.-H.; Chi, C.-C.; Wang, Y.-L. A Study of Trimethylsilane (3MS) and Tetramethylsilane (4MS) Based α -SiCN:H/ α -SiCO:H Diffusion Barrier Films. *Materials* **2012**, *5*, 377–384. [CrossRef] [PubMed]
33. Pech, D.; Schupp, N.; Steyer, P.; Hack, T.; Gachon, Y.; Héau, C.; Loir, A.S.; Sánchez-López, J.C. Duplex SiCN/DLC coating as a solution to improve fretting—Corrosion resistance of steel. *Wear* **2009**, *266*, 832–838. [CrossRef]
34. Ermakova, E.N.; Romyantsev, Y.M.; Rakhlin, V.I.; Kosinova, M.L. Plasma-chemical synthesis of transparent dielectric Si–C–O–H films from trimethylphenoxysilane. *High Energy Chem.* **2016**, *50*, 224–227. [CrossRef]
35. Kramida, A.; Ralchenko, Y.; Reader, J. *NIST ASD Team*; National Institute of Standards and Technology: Gaithersburg, MD, USA, 2022. Available online: <https://search.datacite.org/works/10.18434/t4w30f> (accessed on 15 October 2022).
36. Cui, J.H.; Xu, Z.F.; Zhang, J.L.; Nie, Q.Y.; Xu, G.H.; Ren, L.L. Online diagnosis of electron excitation temperature in CH₄+H₂ discharge plasma at atmospheric pressure by optical emission spectra. *Sci. China Ser. G Phys. Mech. Astron* **2008**, *51*, 1892–1896. [CrossRef]
37. Tauc, J.; Grigorovici, R.; Vancu, A. Optical Properties and Electronic Structure of Amorphous Germanium. *Phys. Stat. Sol. B* **1966**, *15*, 627–637. [CrossRef]
38. Kwok, D.Y.; Neumann, A.W. Contact angle measurements and contact angle interpretation. *Adv. Colloid Interface Sci.* **1999**, *81*, 167. [CrossRef]
39. Owens, D.K.; Wendt, R.C. Estimation of the surface free energy of polymers. *J. Appl. Polym. Sci.* **1969**, *13*, 1741–1747. [CrossRef]
40. Wu, S. *Polymer Interface and Adhesion*; Marcel Dekker: New York, NY, USA, 1982; ISBN 9780824715335.
41. Ivashchenko, V.I.; Porada, O.K.; Kozak, A.O.; Manzhara, V.S.; Sinelnichenko, O.K.; Ivashchenko, L.A.; Shevchenko, R.V. An effect of hydrogenation on the photoemission of amorphous SiCN films. *Int. J. Hydrogen Energy* **2022**, *47*, 7263–7273. [CrossRef]
42. Matsutani, T.; Tai, Y.; Kawasaki, T. Nitrogen ion beam thinning of a-SiCN diaphragm for environmental cell prepared by low-energy ion beam enhanced chemical vapor deposition. *Vacuum* **2020**, *182*, 109770. [CrossRef]
43. Long, D.A. Tables and Charts. In *Infrared and Raman Characteristic Group Frequencies*, 3rd ed.; John Wiley and Sons: Hoboken, NJ, USA; George Socrates: Chichester, UK, 2001. [CrossRef]
44. Langford, A.A.; Fleet, M.L.; Nelson, B.P.; Lanford, W.A.; Maley, N. Infrared absorption strength and hydrogen content of hydrogenated amorphous silicon. *Phys. Rev. B* **1992**, *45*, 13367. [CrossRef] [PubMed]
45. Chagin, M.N.; Sulyaeva, V.S.; Shayapov, V.R.; Kolodin, A.N.; Khomyakov, M.N.; Yushina, I.V.; Kosinova, M.L. Synthesis, Properties and Aging of ICP-CVD SiC_xN_y:H Films Formed from Tetramethyldisilazane. *Coatings* **2022**, *12*, 80. [CrossRef]
46. Kafrouni, W.; Rouessac, V.; Julbe, A.; Durand, J. Synthesis and characterization of silicon carbonitride films by plasma enhanced chemical vapor deposition (PECVD) using bis(dimethylamino)dimethylsilane (BDMADMS), as membrane for a small molecule gas separation. *Appl. Surf. Sci.* **2010**, *257*, 1196–1203. [CrossRef]
47. Wrobel, A.M.; Uznanski, P.; Walkiewicz-Pietrzykowska, A.; Jankowski, K. Amorphous silicon carbonitride thin-film coatings produced by remote nitrogen microwave plasma chemical vapour deposition using organosilicon precursor. *Appl. Organomet. Chem.* **2017**, *31*, e3871. [CrossRef]
48. Khatami, Z.; Bosco, G.B.F.; Wojcik, J.; Tessler, L.R.; Mascher, P. Influence of Deposition Conditions on the Characteristics of Luminescent Silicon Carbonitride Thin Films. *ECS J. Solid State Sci. Technol.* **2018**, *7*, N7. [CrossRef]

49. Khatami, Z.; Mascher, P. Photoluminescence of silicon carbonitride thin films: The interdependence of post-deposition annealing and growth temperature. *J. Lumin.* **2019**, *214*, 116563. [[CrossRef](#)]
50. Uznanski, P.; Walkiewicz-Pietrzykowska, A.; Jankowski, K.; Zakrzewska, J.; Wrobel, A.M.; Balcerzak, J.; Tyczkowski, J. Atomic Hydrogen Induced Chemical Vapor Deposition of Silicon Oxycarbide Thin Films Derived from Diethoxymethylsilane Precursor. *Appl. Organomet. Chem.* **2020**, *34*, e5674. [[CrossRef](#)]
51. Veres, M.; Koós, M.; Tóth, S.; Füle, M.; Pócsik, I.; Tóth, A.; Mohai, M.; Bertóti, I. Characterisation of a-C:H and oxygen-containing Si:C:H films by Raman spectroscopy and XPS. *Diamond Relat. Mater.* **2005**, *14*, 1051–1056. [[CrossRef](#)]
52. Sobczyk-Guzenda, A.; Oleśko, K.; Gazicki-Lipman, M.; Szymański, W.; Balcerzak, J.; Wendler, B.; Szymanowski, H. Chemical structure and optical properties of a-SiNC coatings synthesized from different disilazane precursors with the RF plasma enhanced CVD technique—A comparative study. *Mater. Res. Express* **2019**, *6*, 016410. [[CrossRef](#)]
53. Chang, W.Y.; Chang, C.Y.; Leu, J. Optical properties of plasma-enhanced chemical vapor deposited SiC_xN_y films by using silazane precursors. *Thin Solid Films* **2017**, *636*, 671–679. [[CrossRef](#)]
54. Belmahi, M.; Bulou, S.; Thouvenin, A.; Poucques, L.; Hugon, R.; Brizoual, L.; Miska, P.; Genève, D.; Vasseur, J.L.; Bougdira, J. Microwave plasma process for SiCN:H thin films synthesis with composition varying from SiC:H to SiN:H in H₂/N₂/Ar/Hexamethyldisilazane gas mixture. *Plasma Process. Polym.* **2014**, *11*, 551–558. [[CrossRef](#)]
55. Sinha, A.K.; Lugujo, E. Lorentz-Lorenz correlation for reactively plasma deposited Si-N films. *Appl. Phys. Lett.* **1978**, *32*, 245. [[CrossRef](#)]
56. Swanepoel, R. Determination of the thickness and optical constants of amorphous silicon. *J. Phys. E Sci. Instrum.* **1983**, *16*, 1214. [[CrossRef](#)]
57. Bachar, A.; Bousquet, A.; Mehdi, H.; Monier, G.; Robert-Goumet, C.; Thomas, L.; Belmahi, M.; Goulet, A.; Sauvage, T.; Tomasella, E. Composition and optical properties tunability of hydrogenated silicon carbonitride thin films deposited by reactive magnetron sputtering. *App. Surf. Sci.* **2018**, *444*, 293–302. [[CrossRef](#)]
58. Saito, N.; Goto, T.; Tomioka, Y.; Yamaguchi, T. Improvement of photoconductivity of a-SiC:H films by introducing nitrogen during magnetron sputtering process. *J. Appl. Phys.* **1991**, *69*, 1518–1521. [[CrossRef](#)]
59. Kozak, A.O.; Ivashchenko, V.I.; Porada, O.K.; Ivashchenko, L.A.; Tomila, T.V.; Manjara, V.S.; Klishevych, G.V. Structural, optoelectronic and mechanical properties of PECVD Si–C–N films: An effect of substrate bias. *Mater. Sci. Semicond. Process.* **2018**, *88*, 65–72. [[CrossRef](#)]
60. Nguyen, H.H.; Jayapal, R.; Dang, N.S.; Nguyen, V.D.; Trinh, T.T.; Jang, K.; Yi, J. Investigation of charge storage and retention characteristics of silicon nitride in NVM based on InGaZnO channels for system-on-panel applications. *Microelectron. Eng.* **2012**, *98*, 34–40. [[CrossRef](#)]
61. Honda, K.; Yoshinaga, K.; Nagata, Y. Amorphous Carbon-Based Semiconductor Capable of Controlling Its Optical Gap and Conductivity by Incorporating Silicon and Nitrogen Atoms. *ECS J. Solid State Sci. Technol.* **2016**, *5*, P590. [[CrossRef](#)]
62. Rossi, D.; Landers, R.; Bortoleto, J.R.R.; Durrant, S.F. Characterization of PECVD a-C:H:Si:O:Cl films. *J. Vac. Sci. Technol. A* **2017**, *35*, 04D103. [[CrossRef](#)]
63. Wrobel, A.M.; Walkiewicz-Pietrzykowska, A.; Uznanski, P.; Glebocki, B. a-SiC:H Films by Remote Hydrogen Microwave Plasma CVD From Ethylsilane Precursors. *Chem. Vap. Depos.* **2013**, *19*, 242–250. [[CrossRef](#)]
64. Nogueira, S.; da Silva, M.L.P.; Tan, I.H.; Furlan, R. Production of highly hydrophobic films using low-frequency and high density plasma. *Rev. Bras. De Apl. De Vácuo* **2006**, *25*, 45.
65. Batocki, R.G.S.; Mota, R.P.; Honda, R.Y.; Santos, D.C.R. Amorphous silicon carbonitride films modified by plasma immersion ion implantation. *Vacuum* **2014**, *107*, 174–177. [[CrossRef](#)]
66. Bhaskar, N.; Sulyaeva, V.; Gatapova, E.; Kaichev, V.; Rogilo, D.; Khomyakov, M.; Kosinova, M.; Basu, B. SiC_xN_yO_z coatings enhance endothelialisation, bactericidal and reduce blood cell activation. *ACS Biomater. Sci. Eng.* **2020**, *6*, 5571–5587. [[CrossRef](#)]
67. Mora-Cortes, L.F.; Rivas-Muñoz, A.N.; Neira-Velázquez, M.G.; Contreras-Esquivel, J.C.; Roger, P.; Mora-Cura, Y.N.; Soria-Arguello, G.; Bolaina-Lorenzo, E.D.; Reyna-Martínez, R.; Zugasti-Cruz, A.; et al. Biocompatible enhancement of poly(ethylene terephthalate) (PET) waste films by cold plasma aminolysis. *J. Chem. Technol. Biotechnol.* **2022**, *97*, 3001–3010. [[CrossRef](#)]
68. Choi, Y.; Tran, H.-V.; Lee, T.R. Self-Assembled Monolayer Coatings on Gold and Silica Surfaces for Antifouling Applications: A Review. *Coatings* **2022**, *12*, 1462. [[CrossRef](#)]
69. Zhu, L.; Dikin, D.A.; Percec, S.; Ren, F. Improving Interlayer Adhesion of Poly(p-phenylene terephthalamide) (PPTA)/Ultra-high-molecular-weight Polyethylene (UHMWPE) Laminates Prepared by Plasma Treatment and Hot Pressing Technique. *Polymers* **2021**, *13*, 2600. [[CrossRef](#)]
70. Hegemann, D.; Brunner, H.; Oehr, C. Plasma treatment of polymers for surface and adhesion improvement. *Nucl. Instrum. Methods Phys. Res. B* **2003**, *208*, 281–286. [[CrossRef](#)]
71. Urbanowicz, A.M.; Shamiryan, D.; Zaka, A.; Verdonck, P.; De Gendt, S.; Baklanov, M.R. Effects of He Plasma Pretreatment on Low-*k* Damage during Cu Surface Cleaning with NH₃ Plasma. *J. Electrochem. Soc.* **2010**, *157*, H565. [[CrossRef](#)]
72. Shayapov, V.R.; Chagin, M.N.; Kolodin, A.N.; Kosinova, M.L. Deposition of Films from a Mixture of Hexamethylcyclotrisilazane Vapor and Argon in Inductively Coupled Plasma. *Glass Phys. Chem.* **2019**, *45*, 525–531. [[CrossRef](#)]
73. Racka-Szmidt, K.; Stonio, B.; Żelazko, J.; Filipiak, M.; Sochacki, M. A Review: Inductively Coupled Plasma Reactive Ion Etching of Silicon Carbide. *Materials* **2022**, *15*, 123. [[CrossRef](#)]

74. Kumar, D.; Swain, B.P. Investigation of structural and mechanical properties of silicon carbonitride thin films. *J. Alloys Compd.* **2019**, *789*, 295. [[CrossRef](#)]
75. Zhang, C.; Qu, L.; Yuan, W. Effects of Si/C Ratio on the Phase Composition of Si-C-N Powders Synthesized by Carbonitriding. *Materials* **2020**, *13*, 346. [[CrossRef](#)] [[PubMed](#)]
76. Gray, R.C.; Carver, J.C.; Hercules, D.M. An ESCA study of organosilicon compounds. *J. Electron. Spectros. Relat. Phenom.* **1976**, *8*, 343–357. [[CrossRef](#)]
77. Vassallo, E.; Cremona, A.; Ghezzi, F.; Dellera, F.; Laguardia, L.; Ambrosone, G.; Coscia, U. Structural and optical properties of amorphous hydrogenated silicon carbonitride films produced by PECVD. *Appl. Surf. Sci.* **2006**, *252*, 7993–8000. [[CrossRef](#)]
78. Peng, L.; Kim, S.W.; Iacovo, S.; Inoue, F.; Phommahaxay, A.; Sleenckx, E.; De Vos, J.; Zinner, D.; Wagenleitner, T.; Uhrmann, T.; et al. Advances in SiCN-SiCN Bonding with High Accuracy Wafer-to-Wafer (W2W) Stacking Technology. In Proceedings of the 2018 IEEE International Interconnect Technology Conference (IITC), Santa Clara, CA, USA, 4–7 June 2018; pp. 179–181. [[CrossRef](#)]
79. Son, S.; Min, J.; Jung, E.; Kim, H.; Kim, T.; Jeon, H.; Kim, J.; Kim, S.; Moon, K.; Na, H.; et al. Characteristics of Plasma-activated Dielectric Film Surfaces for Direct Wafer Bonding. In Proceedings of the 2020 IEEE 70th Electronic Components and Technology Conference (ECTC), Orlando, FL, USA, 3–30 June 2020; pp. 2025–2032. [[CrossRef](#)]
80. Ghosh, H.; Mitra, S.; Saha, H.; Datta, S.K.; Banerjee, C. Argon plasma treatment of silicon nitride (SiN) for improved antireflection coating on c-Si solar cells. *Mater. Sci. Eng. B* **2017**, *215*, 29–36. [[CrossRef](#)]
81. Li, D.; Xu, K.; Zhang, Y. A Review on Research Progress in Plasma-Controlled Superwetting Surface Structure and Properties. *Polymers* **2022**, *14*, 3759. [[CrossRef](#)]

Disclaimer/Publisher's Note: The statements, opinions and data contained in all publications are solely those of the individual author(s) and contributor(s) and not of MDPI and/or the editor(s). MDPI and/or the editor(s) disclaim responsibility for any injury to people or property resulting from any ideas, methods, instructions or products referred to in the content.